Civil and Environmental Engineering
Vol. 21, Issue 2, 712-727, DOI: 10.2478/cee-2025-0051

CEMENT TYPE EFFECT ON EARLY AGE CRACK BEHAVIOR OF END-TO-END RESTRAIND REINFORCED CONCRETE BEAM

Yasameen N. K. ALBRESHA [1,*], Hussam K. RISAN[1]

[1] Department of Civil Engineering, College of Engineering, Al-Nahrain University, Baghdad, Iraq.
[*] corresponding author: St.yasmeen.N@ced.nahrainuniv.edu.iq

Abstract

This study investigates the early-age cracking behavior of continuously reinforced concrete beams restrained at their ends. It focuses on casting a 30m-long reinforced beam, utilizing concrete mixes with identical compressive strengths but different cement types. Recent research has overlooked how ambient temperature and internal temperature variations from cement hydration affect crack formation in outdoor environments during the early stages. Consequently, it compares the heat evolution during the early stages for the 30-meter beam against that of a 150mm cube specimen, examining the effects of the two types of cement employed. Test results demonstrate that using sulfate-resisting cement (SRC) results in a more significant occurrence of early-age cracks comparing ordinary Portland cement (OPC), with crack widths 33% to 50% wider for SRC. Additionally, the peak temperature resulting from the cement hydration in the cube specimens was 5 to 6 degrees higher than in the 30 m long beam for both cements. Lastly, Since the fineness of SRC is higher than that of OPC, its compressive strength at 7 days was 8% greater than that of OPC; however, the 28-day strengths were nearly the same.

Keywords:

Reinforced continuous beam;
Early-age cracking;
End-to-end restrained beam;
Hydration of cement;
Sulphate-resisting cement
Hydration.

1 Introduction

Non-structural cracking is a severe problem in concrete, it resulted from the volumetric changes in the early age cast concrete. These changes are caused by heat, cement hydration, creep, shrinkage, and seasonal effects due to environmental conditions. Concrete is seldom unrestrained in practice; these change-restrained movements will induce cracks in the reinforced concrete structures. It is either internally due to reinforcement or externally by adjacent parts of the structure, which either have edges restrained or ends restrained. Even though cracking cannot be eliminated entirely, it can be controlled or reduced to an acceptable extent. Many codes and researchers have studied the early-age cracking of externally restrained concrete members. In 2019, Mushchil et al. [1] studied the control of shrinkage and thermal cracking in the end and base-restrained mortar walls. In outdoor conditions, the reduced-scale walls were cast during summer and winter with different (length/high) ratios. He found that the first crack, the maximum crack width, lies in the center of the wall where the maximum restraint is. Also, it can be controlled by concentrating the horizontal steel reinforcement in this zone. Lastly, the outcome demonstrates that secondary cracks will be induced when the (length/high)ratio is less than 2.5. While increasing this ratio will induce primary and secondary cracks, this complies with AL Mashhadi, M. A.[2], who studied the control of secondary shrinkage on edge-restrained mortar walls. Mohammed et al. [3] studied the shrinkage behavior of base-restrained, high-strength plain concrete walls, as did Mushchil et al [1]. Moreover, Mohammed et al. [3] used different (length/high) ratios. The results demonstrate that cracking occurs when the (length/high) ratio is≥ eight while increasing this ratio above eight will increase the maximum crack width and decrease the maximum shrinkage strain. This conclusion ensures that the internal restraint due to horizontal reinforcement significantly impacts the formation of early-age cracks in reinforced structures, as produced by Kheder G. F.[4] Who investigated the cracking behavior of concrete walls restrained at their bases. Many parameters were studied, such as (length/high) ratio, drying conditions, and horizontal steel reinforcement. However, the result showed that the cracks' spacing and width are always related to the (length/high) ratio and the horizontal steel reinforcement which complies with Matiašková L et al [5]. Matiašková L. et al [5] showed rising L/H has a direct influence on the increasing risk of microcracking deduced from stress resultants. Al Attar, T. S. [6] deeply investigated the horizontal steel reinforcement ratios as well as other secondary parameters in the crack control study on base-restrained members. The study demonstrates that the minimum steel ratio and observed crack width for base-restrained members is smaller than that for end-restrained members because the preposition of the base-restrained acts as an additional reinforcement. Kheder, G. F. Et al [7] studied the cracking of base-restrained reinforced concrete walls due to volume change. The observed primary and secondary crack spacings and widths of some 61 full-size walls and 14 experimental walls demonstrate that since the crack width is not uniform across the wall height, the percentage of reinforcement may vary with the wall height. This variation could lead to savings in reinforcement costs. Wu, C. H. et al [8] investigated early-age interior temperature development of high-strength concrete slabs. The variables were the water/cementitious ratio and the cement replacement ratio of silica fume and fly ash. The results showed cracking occurs within 4 hours after casing for the slabs with a water/cementitious ratio ranging (from 0.25 to 0.4). Increasing the silica fume amount as a cement replacement will increase the maximum central temperature of the slab.

Other researchers studied the behavior of early-age movement using finite element base programs such as ABAQUS, ANSYS, etc. AL-Zuhairi, A. H. A [9] studied cracking behavior and stress analysis of mass concrete structures due to temperature variation and drying shrinkage volume changes using two computer programs (FORTRAN and ANSYS). For maximum crack width and the development of strains and stresses in the fixed-end walls, the results showed agreement with the estimated results using the procedure proposed by ACI Committee 207. In the same concept, Risan, H. K. [10] showed a good agreement between the results of the ANSYS program and the proposed procedure by the British standard codes when he studied the cracking behavior in watertight continuous structures. Bilčík et al. [11] demonstrate that temperature changes primarily cause early-age cracks in massive slabs. There is a notable gap in research concerning the variations in internal temperatures of concrete in situ resulting from the cement hydration process and its effects on the early-age crack behavior of reinforced concrete members.

Lastly, Previous researchers investigated the temperature evolution associated with the hydration of cement in concrete [12-16], using standard laboratory tests under adiabatic conditions as a material characteristic. In contrast, some evaluate the thermal evolution of structural components, including slabs [8] and constrained walls [17], in controlled laboratory environments. Additionally, some researchers have employed finite element modeling (FEM) techniques to simulate temperature variation fields [18]. This study examines the crack behavior of a 30-meter-long end-to-end restrained beam cast outdoors during the summer. The cracking behavior of reinforced concrete elements at an early age is significantly affected by fluctuations in environmental temperature, particularly in hot climates, as demonstrated by summer conditions in Iraq. The recent paper evaluates the variations in the inner temperature of concrete under outdoor conditions to assess the influence of actual environmental factors on the evolution of hydration temperature and, consequently, how these variations contribute to the early-age formation of cracks in reinforced concrete structures.

2 Experimental work

2.1 Material

The reinforced concrete beams were cast with 33 and 32 MPa cubic compressive strength. Ordinary Portland cement and sulfate-resistance cement were used to produce two different mixes with almost the same compressive strength.

- Both O.P.C. and S.R.C. comply with the requirement of EN 197[37]. The chemical and physical properties are presented in Table 1.
- The sand was a well-rounded natural material with a fineness modulus of 2.96, specific gravity of 2.63, and Sulfate (SO_3) content of 0.365%.
- The coarse aggregate has a maximum size of 17 mm, a specific gravity of 2.55, water absorption of 0.48%, and 0.087% sulfate(SO_3) content. Sieve analysis of the fine and coarse aggregate is shown in Tables 2 and 3.
- Deformed steel bars of 12 mm diameter were used. The average yield strength of the three samples is 422 MPa. The used steel reinforcement ratio was 0.003 for all models, which is larger than the minimum steel ratio according to BS 8007 [31], BS EN 1992-1[32], and ACI 318-11.

Concrete mixes were prepared using an electric mixer to ensure uniformity. The dry components—cement, sand aggregate, and coarse aggregate—were blended until a consistent color was achieved, followed by adding water. Mixing concrete lasted 3 to 5 minutes to ensure proper consistency. Two different cement types were used to produce the concrete mixes: ordinary Portland cement (OPC) and sulfate-resisting cement (SRC). The concrete mix made with ordinary Portland cement (OPC) represents the reference mix in this paper.

A single batch was used to cast four reinforced concrete beams and their corresponding control specimens, which included six cubes for compressive strength (150x150) mm, six cubes for heat of hydration (150x300) mm, nine cylinders (150x300) mm for splitting tensile strength, and six cylinders (150x300) mm for compressive strength. Additionally, three prisms (100x100x400) mm were prepared for modulus of rupture testing. The beams were cast in molds and compacted with an electric vibrator.

Table 1: Chemical and physical properties of the used cement [38].

Chemical compositions [%]	O.P.C. content	S.R.C. content
Chemical properties:		
C_3A	6.31	2.21
MgO	2.49	2.67
SO_3	2.29	2.09
Loss on ignition [%]	2.45	2.66
Insoluble residue [%]	0.73	0.64
Physical properties:		
Blaine fineness [cm^2/kg]	3154	3394
Initial setting time [min]	114	115
Final setting time [hr: min]	2:42	2:51
Compressive strength [MPa]:		
2 days	25.7	25.6
28 days	46.5	46

Table 2: Sand grading according to Iraqi specifications [38].

Sieve size [mm]	Passing [%]	Limit of Iraq specification
4.75	97.4	90–100
2.36	75	75–100
1.18	68.6	55–90
0.6	40.3	35–59
0.3	28.2	8–30
0.15	2.1	0–10

Table 3: The grading of coarse aggregate according to Iraqi standards[38]

Sieve size [mm]	Passing [%]	Limit of Iraq specification
20	100	100
14	91	100–90
10	81	85–50
5	5	50–0
2.36	0	–

2.2 Continuous end-restrained beam casting

End-to-end constrained reinforced concrete strip beams were cast outside during the summer (July) to emulate natural environmental conditions. This study used two different concrete mixes to examine their influence on the early-age cracking behavior of the tested models. Each mix was cast with four identical beams. The beams, 30 meters long and (150x150) mm in cross-section, were reinforced with a single steel bar in the canter. The moulds for casting the four beams for each concrete mix were constructed using 18 mm thick plywood. The major parameter of this study was the type of cement used. The details of formwork and casting are seen in Figure 1.

2.3 Curing and exposure

Following the casting, polyethylene sheets were used to cover the upper surfaces of the beams and control specimens. This precaution minimizes the risk of plastic shrinkage cracking, which can occur due to rapid evaporation under specific conditions. Once the moulds were removed, the beams were cured by covering them with wet canvas. It was moistened daily for five days to ensure the concrete retained adequate humidity during its early curing stages. Subsequently, the beams were allowed to air dry in uncontrolled laboratory and outdoor settings, subjecting them to diverse atmospheric conditions.

Observations were conducted to monitor the development of cracking, facilitating an understanding of the concrete's behaviour over time.

Interestingly, plastic shrinkage cracking was first observed in the continuous beams made with SRC cement just one day after casting. However, this early occurrence is not a primary concern of the current study, so it wasn’t considered. Table 4 and Figure 2 detail the conditions recorded for each set during the casting process.

Table 4: The casting details.

Notation	Time of mixing start	Time start record	The temperature of concrete at placing	Weather temperature	Relative humidity [%]
C-OPC	3:45 pm	6:00 pm	29	44	20
C-SRC	1:00 pm	2:00 pm	28	46	20
*c: referred to continuous beams, OPC: ordinary Portland cement, SRC: sulfate-resisting cement.					

Fig. 1: a) The formwork, b) during casting, c) leveling the surface, d) and e) after casting, d) the hardened 30m beams.

Fig. (2): The weather details during the casting.

2.4 Measurements of strain, crack Width, and heat of hydration

- Strain measurement: Strain gauges attached to the beams' midpoints were used to measure the concrete and steel reinforcing strains. At the center of the beam, two different strain gauges were installed: a 3 mm strain gauge on the reinforcing bar and an 8 cm strain gauge on the concrete surface. The reinforcing rebar was first flattened by eliminating the distorted ribs and properly cleaned. The strain gauges were then bonded with a specialized adhesive and wrapped with water-resistant tape to avoid moisture absorption during concrete placement, see Figure 3. Two days after de-moulding, the 8 cm strain gauge was affixed to the polished and cleaned surface of the concrete and then coated with epoxy to reduce moisture absorption, see Figure 4.
- Crack width measurements: a portable microscope with 40X magnification (crack meter) was used to measure the crack width, which has a measuring field of 4 mm (see Figure 4).
- The heat of hydration measurements techniques: a thermistor was employed to monitor the internal temperature development of the concrete members, as did Wu, C. H. [8]. This technique was used to evaluate the temperature evolution during the hydration process for the beams and the control specimens by using a self-developed data logging system that recorded the strain and temperature data every second.:

1) Continuous concrete beam technique: The thermistor was embedded in the center of the middle length of the 30 m beam, as shown in Figure 5. After casting, the heat evolution was recorded using the data logger for almost four days.

2) cube control specimens technique: the thermistor was embedded in the center of the (150x150)mm cube, and 18 mm plywood was used to make the 150mm-cube, as shown in Figure 6 to compare the inner heat development with the continuous strip beams

It should be noted that no researcher or study has investigated the heat of the hydration process from this point of view, nor have the techniques described above been used. This study aims to clearly illustrate how the volume and dimensions of a structure influence the amount of heat generated during the hydration of cement in practical circumstances. Furthermore, it will explore the significant role that ambient temperature plays in this process, mainly how it affects the release and dissipation of heat over time.

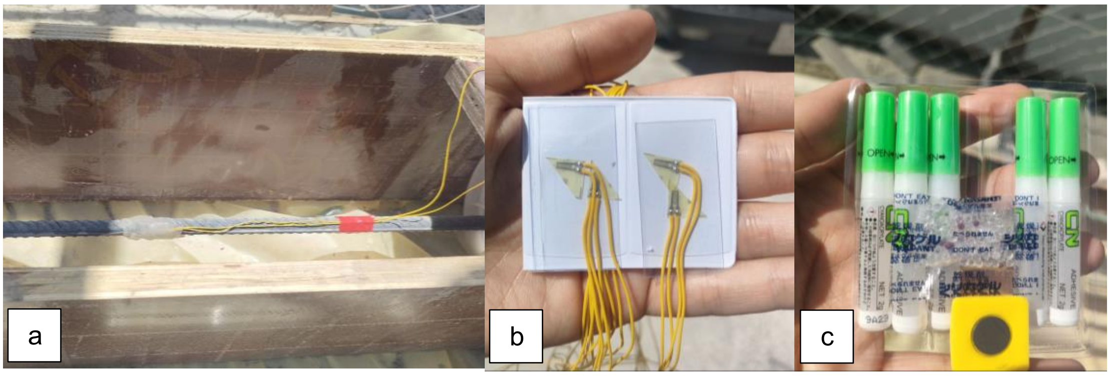

Fig. 3: a) strain gauge installing, b) the 3 mm strain gauge, d) the used adhesive.

2.5 Mechanical Properties Tests

- The compressive strength of concrete: The compression strength test was carried out on 7, 28 days water cured (150mm) cubes according to BS EN 12390-3[36] and (150x300)mm cylinder concrete according to *ASTM C39* [34]. As shown in Figure 7.
- The tensile splitting strength: tensile strength test was carried out on 3,7, and 28 days cured concrete cylinder with dimensions of (150x300) mm according to ASTM C496[33]. As shown in Figure 7.
- The modulus of rapture: the test was carried out on 28 days of cured concrete prism with dimensions of (100x100x400) mm according to the procedure of ASTM C78 [35] shown in Figure 7. All the tests mentioned were applied for the two mixes present in Table 5.

Table 5: Mixes constituents.

Mixes constituents [kg/m^3]	M1-OPC	M2-SRC
Cement [kg/m^3]	350	350
Fine aggregate [kg/m^3]	950	950
Coarse aggregate [kg/m^3]	1050	1050
W/C ratio	0.44	0.45
Slump [mm]	70	75

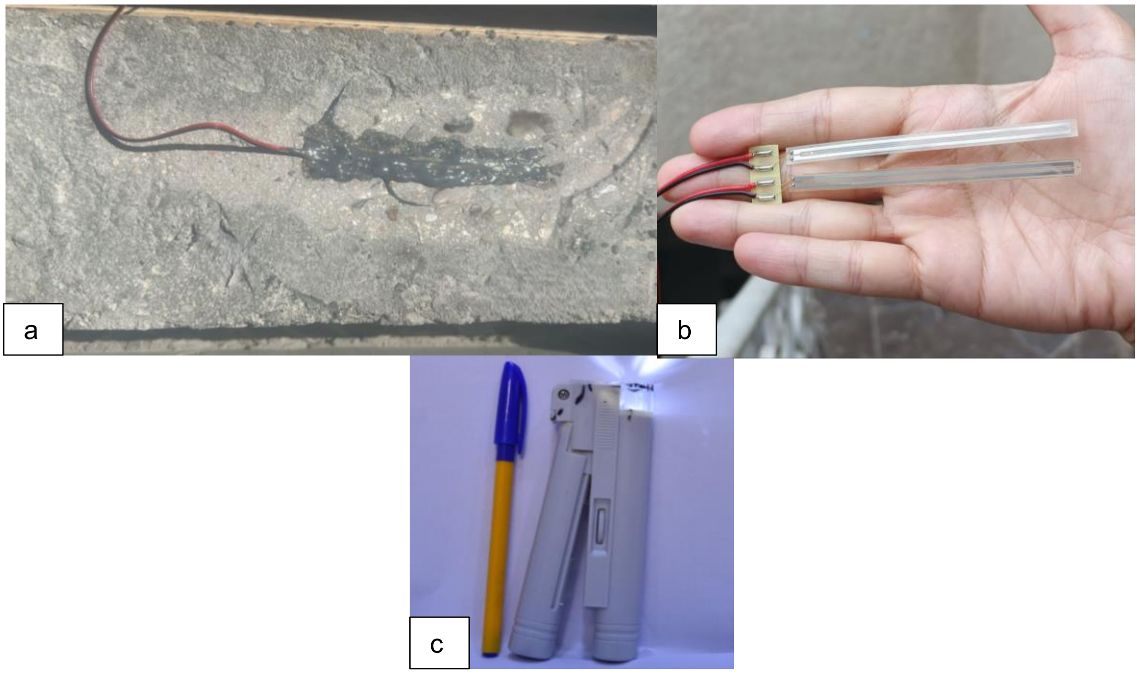

Fig. 4: a) Strain gauge installing, b) the 8 mm strain gauge, d) crackmeter.

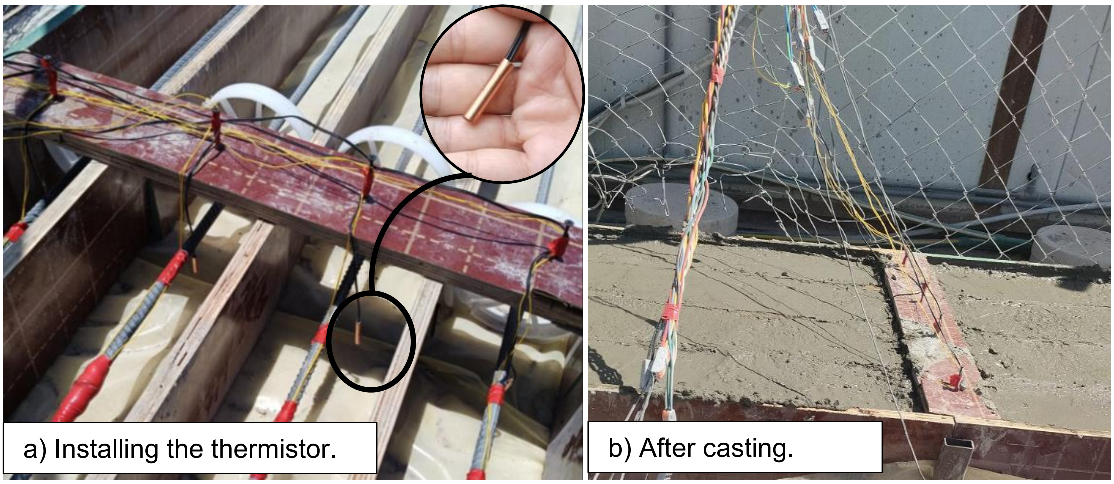

Fig. 5: The thermistor installed in the 30-length beams.

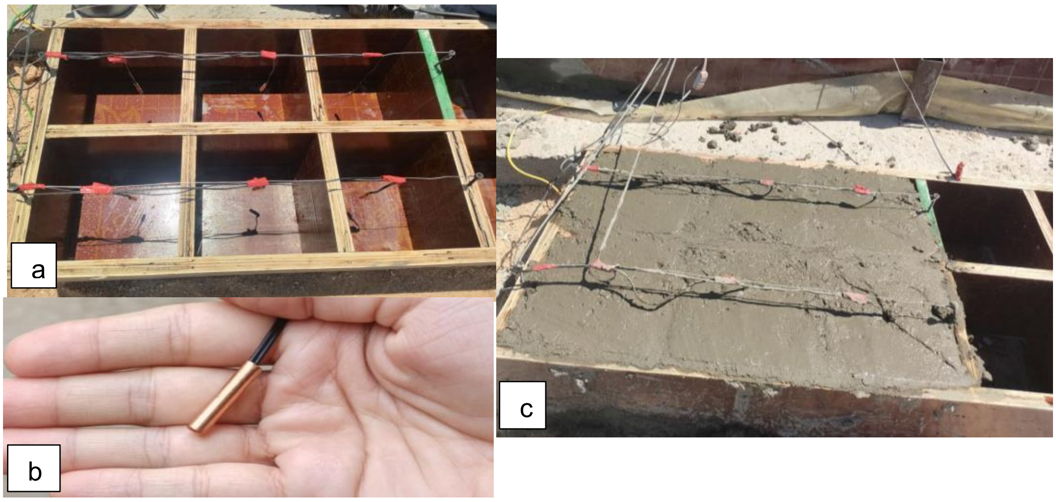

Fig. 6: a) The thermistor installing, b) the thermistor, d) after casting.

3 Results and discussion

3.1 Mechanical properties of concrete mixes

Table 6 shows the mechanical properties of concrete for (M1-OPC) and (M2-SRC) control specimens. Each value in the mentioned table is the average of the results of three different samples for each mix. Figure 7 clarifies the failure patterns observed in the tested specimens.

Table 6: The mechanical properties.

Mixes notation	Cubic compressive strength [MPa]		Cylindrical compressive strength [MPa]		Split tensile strength [MPa]			Flexural strength [MPa]
	7-days	28-days	7-days	28-days	3-days	7-days	28-days	28- days
M1-OPC	22.07	33.1	13.65	25.6	1.63	2.2	2.72	2.4
M2-SRC	24.4	32.2	14.56	24.5	1.72	2.32	2.78	2.46

Modulus of rapture

Split tensile strength

Cubic compressive strength

Fig. 7: Control specimens failure modes.

Table 6 shows that the cylinder's 28-day compressive strength is 0.77 times that of the cube. This finding aligns with the values recommended by ASTM, which indicates that the compressive strength derived from a cylinder is generally around 0.8 times that of a cube.

Although the compressive strength of the mixtures using (M1-OPC) and (M2-SRC) was equivalent initially, the difference became more pronounced after seven days of curing. The 8% increase in strength can be attributed to the fineness of SRC cement, which speeds up the hydration process and accelerates the formation rate of hydration products compared to OPC. This observation aligns with Neville's findings [21], which highlight that the degree of cement hydration is a critical factor in strength development. Furthermore, the split tensile strength measured after 3 days demonstrates a similar trend, although the difference is minimal, which can be explained by the same factors previously discussed.

The results of the other mechanical parameters of the concrete mixtures reveal amazing homogeneity, devoid of inconsistencies or variations. This is in addition to the compressive strength of the concrete mixtures. This dependability highlights the consistency of the material's performance.

3.2 Temperature distribution of NSC beams:

The cracking behavior of reinforced concrete elements at an early age is significantly affected by fluctuations in environmental temperature, particularly in hot climates, as demonstrated by summer conditions in Iraq. The recent paper evaluates the variations in the inner temperature of concrete under outdoor conditions to assess the influence of actual environmental factors on the evolution of hydration temperature and, consequently, how these variations contribute to the early-age formation of cracks in reinforced concrete structures.

All specimens within a single set exhibited analogous internal temperature fluctuations; thus, the mean of the recorded values for each set was employed in Figure 8 to analyze the internal temperature variation immediately post-casting and over four days for the beams and control specimens.

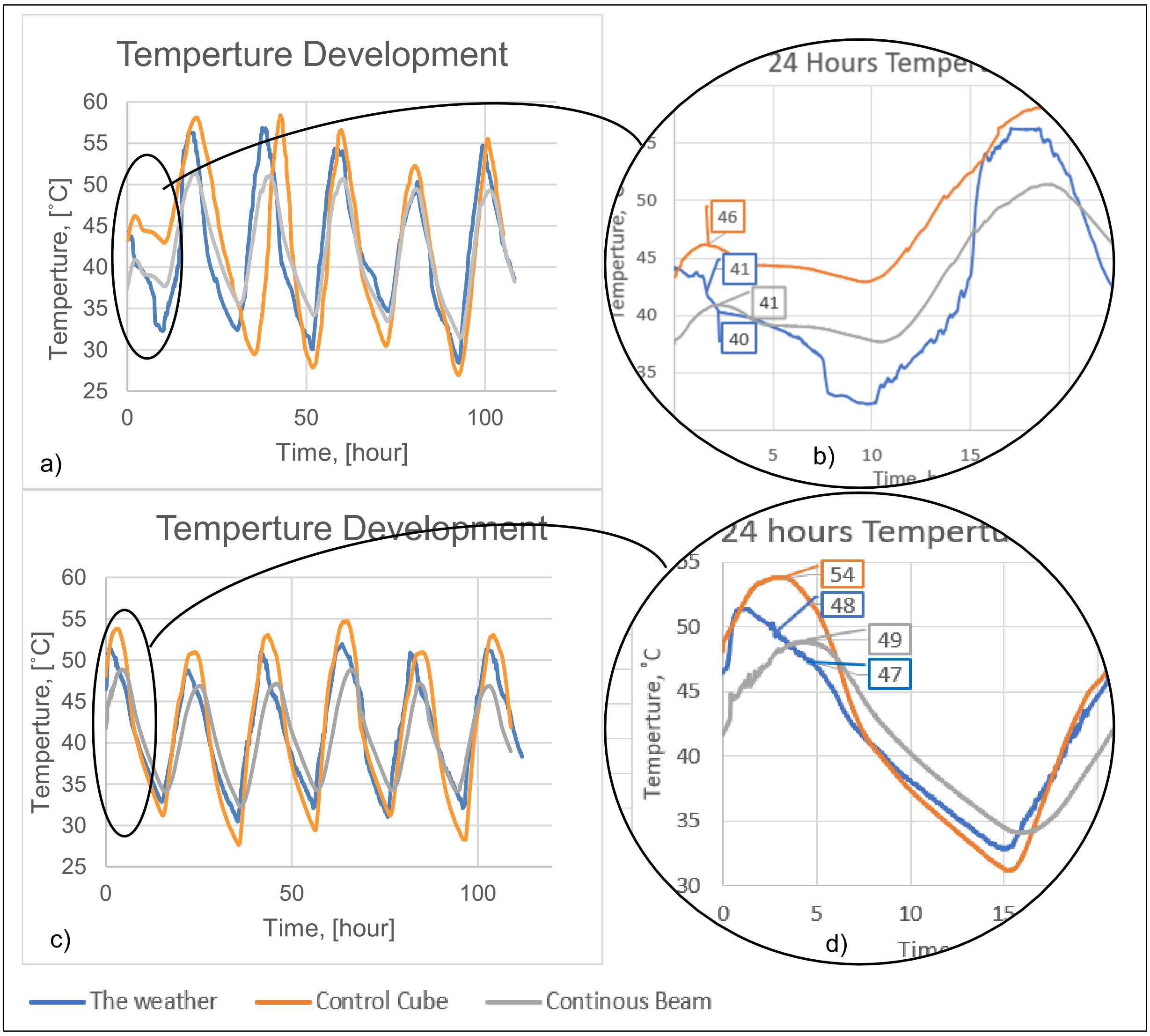

Fig. 8: The temperature-time curves for a) C-OPC, b) C-OPC during the hydration process only, c) C-SRC, d) C-SRC during the hydration process only.

A general trend has been identified in the analysis of Figure 8, indicating that both the continuous beams and the control specimens initially experienced a rise in internal temperature due to hydration heat, thereafter declining to be near ambient values. Nonetheless, their thermal behavior exhibited notable changes with the ambient temperature. Even though the cross-sectional area of the 30-meter beam and the cube is identical, the square 150mm. During the day, the cube's interior temperature has remained higher than the atmospheric temperature, but at night, it drops below. So far, this pattern has shown a rapid temperature response; this might be because the cube has a lower volume-to-surface area ratio. Conversely, the internal temperatures of the elongated beam exhibited an inverse trend, remaining lower than the ambient environment during the day and slightly higher at night. This indicates that the beam length induces a thermal lag due to the slower dissipation of heat over extended distances. This delay indicates that the beam may not warm at the same rate as the cube during the day, resulting in its temperature remaining lower than that of the ambient weather. Nonetheless, the beam retains residual daytime heat at night due to gradual dissipation along its considerable length, frequently resulting in a higher temperature than the surrounding night air. This indicates that a significant quantity of internal heat must travel a longer distance to exit the environment, whereas the cube provides shorter pathways for the internal heat to dissipate through all surfaces. These varied thermal behaviors in various geometric configurations demonstrate how structural shape (in the case of the recent paper, the beam length) affects temperature progress and, consequently, the early crack formation under real ambient conditions. This complies with [19] [20], showing the high importance of the structure volume and the weather effect.

In analyzing the generated heat during the hydration phase Figure 7b and d, a significant difference was observed between the continuous concrete beams using sulfate-resistant cement (SRC) and those utilizing ordinary Portland cement (OPC). The C-SRC reached its maximum temperature of 49 °C, approximately 2°C above the ambient temperature, measured 5 and 40 minutes after mixing. Slightly longer, the M1-OPC mix attained its peak temperature of 41 °C after about 4 hours and 45 minutes, remaining approximately 1 °C above its respective ambient conditions. This means the M2-SRC mix required longer to reach a higher peak temperature during hydration, particularly when subjected to elevated ambient temperatures, compared to the M1 mix. Furthermore, the delayed and somewhat higher peak temperature of the SRC mix may be explained by its slower hydration process due to its lower C3A content, thus the hydration process of SRC cement occurs more gradually until reaches its higher peak temperature compared to OPC. In addition, the high ambient temperature can also be attributed to increasing heat generation. The prolonged hydration period could still result in internal thermal stresses, potentially leading to cracking, especially in large pours where temperature gradients present a challenge. Overall, the results affirm the combined effect of cement type and environmental factors on the development of hydration temperature and the early age behavior of reinforced concrete members under different ambient conditions, which was approved by Neville A. M. [21].

Unlike the control cubes for both concrete mixes, the average peak hydration temperature of the control cubes was approximately (5 to 6) degrees higher than that of the concrete beams. Furthermore, the concrete beams took almost one hour longer to reach their maximum hydration temperature than the control cube for the same set, indicating a significant difference in the thermal behavior during the hydration process. In contrast to the cube, which has a smaller volume, it reaches a higher peak temperature quickly as hydration occurs. After peaking, it cools more rapidly by releasing heat from multiple surfaces simultaneously.

Lastly, as shown in the figure the peak heat rate of the reinforced concrete strip beams was achieved between (5 to 6) hr after mixing which complies with Bentz, D. P. [22]. While other research addressed that the peak hydration may reach between 1 to 3 days [23, 24], this is mainly because the casting was outside in summer weather, the volume of concrete members, the cement content, Concrete temperature, and air temperature [17, 25, 26].

Table 7: Details for maximum temperature of hydration for the concrete beams

The beams	Maximum hydration temperature of the beam (ave.)	The weather temperature	Time after casting	Maximum control specimen's temperature (ave.)	The weather temperature	Time after casting
C-OPC	41°C	40°C	4hr and 45 min.	46°C	41°C	3hr and 50 min.
C-SRC	49°C	47°C	5 hr and 36 min.	54°C	48°C	4 hr and 12 min.

3.3 End Restrained movement: Strain of concrete and steel cracking of continuous beam

The restrained movement of the concrete and the strain of the embedded bar reinforcement (at the middle length of 30m) were acquired from the data logger for each set of the two mixes, as well as the chronological development of the internal temperature of the beams and control specimens. Reading data were recorded every second for each beam using the data logger to investigate the effect of the end-to-end restrained beam with the different concrete mixes on the final crack pattern. The mean data for each set were drawn as presented in Figures 9 and 10.

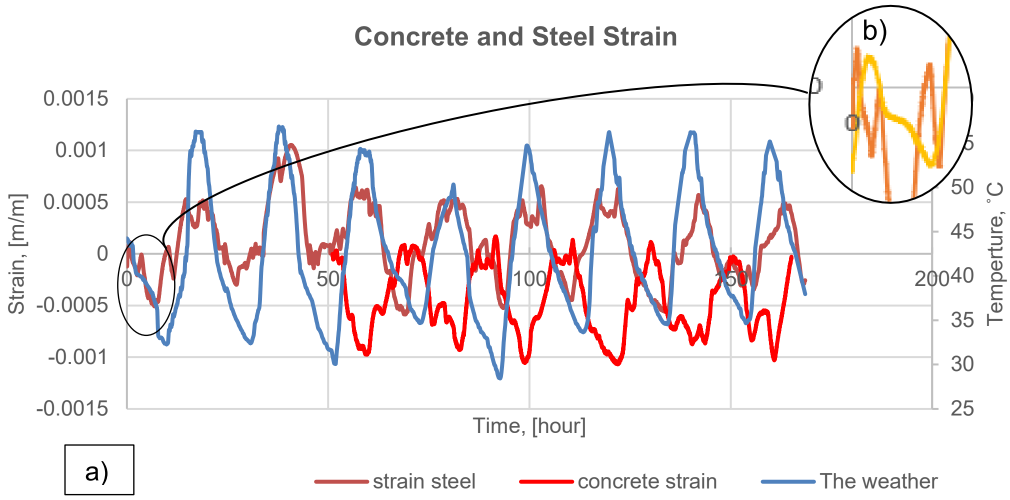

Fig. 9: a) The strain, weather temperature versus time for C-OPC, b) The variation of steel strain due to changes in concrete temperature from the hydration process.

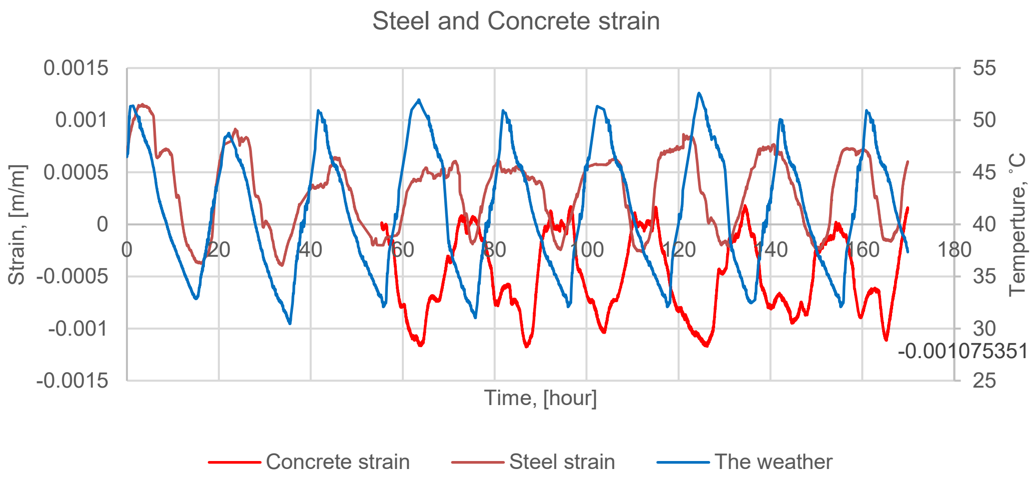

Fig. 10: The strain, weather temperature versus time for the C-SRC.

In General, the international standard codes (ACI 207.2R-07[30], Eurocode 2: EN 1992-1-1[32], and BS 8007[31]) state that as the concrete components are mixed and then poured into molds, the concrete temperature rises due to the hydration of the cement. Then it reaches its peak temperature between 1 to 3 days, depending on several factors (i.e., structure dimension, environment, cement content, etc.). The current paper completed the hydration process within the first day. When it cools and reaches ambient temperature, it hardens and shrinks. The steel is therefore put into compression and the concrete into tension, with longitudinal bond forces present on the surface of the reinforcement. This trend has been approved in Figures 9 and 10, the concrete experiences tension strain due to shrinkage, indicated by the negative value of the strain, which suggests that the concrete is attempting to shorten. In contrast, the strain within the steel is primarily positive, which suggests that it effectively counteracts the shrinkage occurring in the concrete. This interaction leads to a compressive state in the steel

Figures 9 and 10 clearly show that the steel strain was recorded immediately after casting. In contrast, the measurements of concrete strain were taken after a few days and continued thereafter. This delay was due to the experimental procedure, where the concrete was cast, allowed to harden, and then cured. Although specific strain data was not initially available during the first two days, the observed steel strain revealed significant trends related to changes in concrete temperature and environmental conditions.

During hydration, the exothermic reaction of cement hydration generates heat, causing the concrete temperature to rise above the ambient level—approximately 1 degree higher than the external weather. This increase in concrete temperature had a significant effect on the behavior of the steel strain; even minor temperature variations between the concrete and its surroundings could induce strain in the embedded steel. As illustrated in Figure 9a, a small rise in steel strain was observed when the concrete reached its maximum temperature, even though the recorded strain values remained relatively low.

Once the concrete temperature began to decrease toward ambient levels, the concrete started to reach its final set and harden. During this period, the strain in the steel shifted to a positive strain and continued to increase as the ambient temperature rose. This change indicates that as the concrete began to shrink, it induced compressive forces within the steel, highlighting the effects of early-age thermal variation effect on the cracking behavior of reinforced concrete members.

The strains of concrete and steel became more noticeable as they exhibited opposite behaviors, as stated in Figure 9. It shows that negative strain values indicate that the concrete was shrinking and shortening, while positive values in the steel strain reflect that it was stretching in response to this shrinkage. This trend remained similar throughout the majority of the day and night, with the strain on the concrete decreasing during the cooler temperatures of the evening and increasing during the warmer temperatures of the daytime. The concrete's movement induced a similar but opposing trend in steel strain. Nearly all concrete strain values remained negative throughout the testing period, with only a few positive values observed at night due to lower temperatures. This indicates that the beam was continuously experiencing shrinkage. The average maximum recorded strain during the daytime was 0.0011 mm/mm, indicating a significant tendency for the concrete to crack as it shrinks until the end of the test period.

The C-SRC beams showed a notable variation in strain of steel reinforcement behavior. A thorough comparative analysis of the results, illustrated in the accompanying Figure 10, reveals significant discrepancies in the curves that characterize the different materials.

During the SRC's hydration phase, the concrete's internal temperature rose considerably, leading to a marked increase in the steel strain. Specifically, the temperature reached an impressive 46 degrees Celsius during this process, resulting in a higher thermal strain within the C-SRC beams compared to C-OPC beams. As the hydration heat dissipated and the internal temperature began to decrease, a corresponding reduction in strain was observed.

In terms of the concrete strain itself, it was noteworthy that the concrete continued to experience tensile strain even during the nighttime when temperatures typically dropped. Mushchil, A. K. A., et al [1] has corroborated this phenomenon, employing an extensometer to investigate the effects of base and end restraint walls, recording one measurement each day for 2 months. The recent research provides valuable insights into the thermal behavior of concrete in various environmental conditions.

3.4 Cracking age and sequence:

As a rule of thumb, primary cracks in restrained members develop at sections with the highest degree of constraint. In a continuous beam, this generally occurs at the center, where the first crack is induced. Once this initial crack forms, the degree of restraint decreases to zero, leading to a new distribution of restraint. Consequently, the highest degree of restraint will shift to the centerline of the newly formed two halves of the beam, resulting in the formation of additional cracks in these positions.

Between the primary cracks, a group of secondary cracks may develop, potentially increasing in length and width, which could eventually lead to the formation of another primary crack. Plastic shrinkage cracks were initiated in the OPC group at the right side of the beam, This type of crack wasn't given any importance in this paper. Figures 11 and 12 present the crack pattern for the tested C-OPC and C-SRC beams.

CL: centerline.

Fig. (11): the crack pattern for the C-OPC beams set.

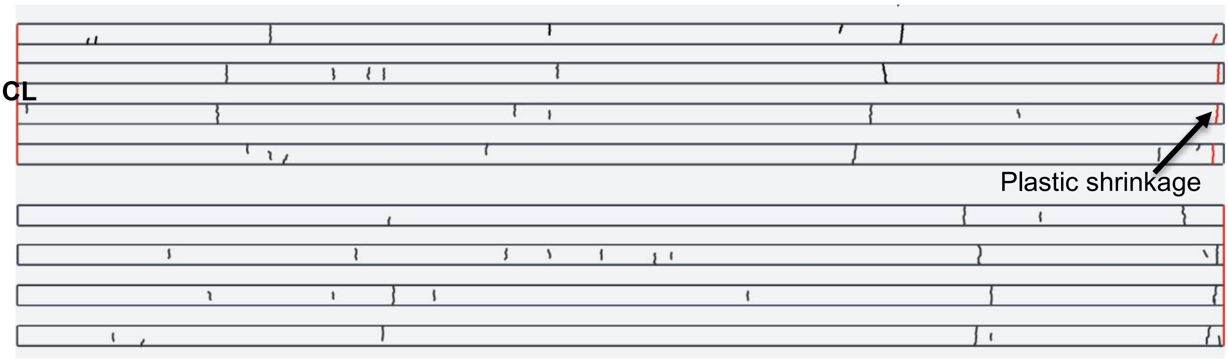

The red cracks represent the plastic shrinkage cracks, CL: centreline

Figure (12): the crack pattern for the C-SRC beams set.

The C-SRC beams showed a wider, larger spacing, and a higher number of cracks than the C-OPC beams; meanwhile, the general crack patterns were similar. As shown in Figure 12 and Table 8.

3.5 Crack spacing and width

For the investigated continuous beams, the spacing and width of primary cracks for the two sets were observed and produced in Table 8. The focus of the recent research on the primary crack because of its propagation through the full width of the studied beam otherwise it is called secondary, which in turn puts the structure's integrity and durability are at risk.

Early age crack, crack width =0.5mm.

Early age crack pattern for the beam.

Similar pattren for the 4 beams (C-SRC)

Fig. 13: Early age cracks in the tested beams.

The fourth C-OPC beam was omitted due to construction issues during casting, leaving only three beams to be considered. During the observation of the C-OPC, the three beams showed almost similar crack spacing and width trends. The observed primary cracks were equal in width (0.5 mm) at an average maximum spacing equal to 6.97m. Figure 12 demonstrates how the total early age strain was either distributed for small closely spaced cracks or wider cracks at large spacing as stated by Forth, J. P. Et al [27]. Meanwhile C-SRC group produced the primary crack width varied widely across all four beams, ranging from (0.5 to 1)mm, the space between cracks was different because the number of cracks was higher than the C-OPC. This variation is attributed to the high internal temperature of the concrete, which is caused by the hydration of cement, as illustrated in Figures 7c and d. The increase in temperature leads to higher strain, resulting in cracks occurring whenever and whatever the concrete's tensile stress reaches its tensile strength. Additionally, the crack width is influenced by the difference in restraint movement before and after cracking (in fact, the crack width is a function of the change in restraint along the beam) as stated by [27,28,29]. Figure 9 shows how the strain of the concrete changes during the observation period and the variation in the strain.

Table 8: Cracks numbers, maximum and minimum crack spacing, and maximum crack width.

Notation.		No. Of cracks	Observed spacing of primary cracks		Max. crack width [mm]	Average observed spacing [m]	Average crack width [mm]
			Min. [m]	Max. [m]			
C-OPC	1	Neglegted				6.969	0.5
	2	3P+7S	5.95	7.75	0.5		
	3	3P+8S	4.35	8.77	0.5		
	4	3P+7S	4.23	4.52	0.5		
C-SRC	1	4P+6S	3.22	7.56	1	9.08	0.8125
	2	4P+12S	2.77	8.13	0.5		
	3	5P+7S	2.82	9.98	1		
	4	3 P+11S	3.16	10.65	0.75		

4. Conclusions

An experimental study was conducted on a 30-meter reinforced concrete beam to investigate the influence of different types of cement on the occurrence of early-age cracking. The research also aimed to understand how ambient temperature variations impact these cracks during the early age of concrete. Extensive analysis of the data and findings presented the following conclusion:

1) For the same steel ratio, using the sulfate-resistance cement will produce a wider crack and a higher number of cracks compared with using the ordinary Portland cement

2) within each group, there was a slight difference between the 4 beams in terms of crack width, crack spacing, number of primary and secondary cracks, and crack pattern. This is because of random variations in the properties of the in-situ concrete.

3) The hydration process of sulfate-resistant cement takes a longer period to generate a higher temperature in concrete compared to the hydration of Portland cement

4) Using a steel reinforcement ratio larger than the minimum steel ratio will not prevent early-age cracks but it may produce a smaller number with a large spacing

5) This study provides valuable insights that can enhance the durability and longevity of concrete structures by guiding best practices in material selection and construction techniques. The characteristics and proportions of materials used in concrete significantly influence the behavior of concrete structures (39)(40)(41).

References

[1] MUSHCHIL, A. K. A., HABEEB, G. M., & AL-MASHHADI, M. S. (2019). Control of shrinkage cracking in end restrained reinforced concrete walls. *architecture (ija)*, *5*(2), 41-62.

[2] AL MASHHADI, M. S. A., 1989. ”Control of secondary shrinkage cracking in reinforced concrete walls”, M. Sc. thesis, college of Engineering, Baghdad University.

[3] MOHAMMED, T. J., AL-TAMEEMI, A. A., & ATTIYAH, A. N., 2018. Cracking Behavior of Base Restrained High Strength Plain Concrete Walls Due to Shrinkage.

[4] KHEDER, G. F. (1986). *Control of shrinkage cracking in reinforced concrete walls* (Doctoral dissertation, MSc thesis, University of Baghdad).

[5] MATIAŠKOVÁ, L., BILČÍK, J., & ŠOLTÉSZ, J. (2018). Control of early-age cracking in watertight concrete structures. *Slovak Journal of Civil Engineering*, *26*(3), 16-21.

[6] AL ATTAR, T. S. (1988). *Minimum steel reinforcement for control of cracking due to shrinkage and temperature changes in reinforced concrete tension members* (Doctoral dissertation, M. Sc. thesis, college of Engineering, Baghdad University).

[7] KHEDER, G. F., AL-RAWI, R. S., & AL-DHAHI, J. K. (1994). A study of the behaviour of volume change cracking in base restrained concrete walls. *Materials and Structures*, *27*, 383-392.

[8] WU, C. H., LIN, Y. F., LIN, S. K., & HUANG, C. H. (2020). Temperature development and cracking characteristics of high strength concrete slab at early age. *Struct. Eng. Mech*, *74*(6), 747-756

[9] AL-ZUHAIRI, A. H. A., (2005) Control of Volume Change Cracking In Plain And Reinforced Massive Concrete With Different Base Restraints, PhD thesis, college of Engineering, Baghdad University.

[10] RISAN, H. K. (2017). Cracking Control Due to Early Thermal Movement of Watertight Continuous RC Members. *Al-Nahrain Journal for Engineering Sciences*, *20*(1), 206-213.

[11] BILČÍK, J., SONNENSCHEIN, R., & GAŽOVIČOVÁ, N. (2017). Causes of early-age thermal cracking of concrete foundation slabs and their reinforcement to control the cracking. *Slovak Journal of Civil Engineering*, *25*(3), 8-14.

[12] DO, T. A., HOANG, T. T., BUI-TIEN, T., HOANG, H. V., DO, T. D., & NGUYEN, P. A. (2020). Evaluation of heat of hydration, temperature evolution, and thermal cracking risk in high-strength concrete at early ages. *Case Studies in Thermal Engineering*, *21*, 100658.

[13] BENTZ, D. P. (2009). Early-age cracking review: mechanisms, material properties, and mitigation strategies. *Current Understanding of the Parameters that Influence Hydraulic and Leaching Properties and Uncertainty Analysis of Cementitious Barriers*, *901945*.

[14] BENTZ, D. P., BENTZ, D. P., JONES, S. Z., PELTZ, M. A., & STUTZMAN, P. E. (2015). *Influence of internal curing on properties and performance of cement-based repair materials*. US Department of Commerce, National Institute of Standards and Technology.

[15] BALLIM, Y., & GRAHAM, P. C. (2003). A maturity approach to the rate of heat evolution in concrete. *Magazine of concrete research*, *55*(3), 249-256.

[16] SCHINDLER, A. K., & FOLLIARD, K. J. (2003, August). Influence of supplementary cementing materials on the heat of hydration of concrete. In *Advances in cement and concrete IX conference, copper mountain conference resort in Colorado*.

[17] MICALLEF, M., VOLLUM, R. L., & IZZUDDIN, B. A. (2017). Cracking in walls with combined base and end restraint. *Magazine of Concrete Research*, *69*(22), 1170-1188.

[18] TAN, Y., & TANG, K. (2024). Modelling In Situ Concrete Temperature Development: The Impact of Ambient Temperature and GGBS Replacement. *CivilEng*, *5*(3), 694-716.

[19] YUAN, Y., & WAN, Z. L. (2002). Prediction of cracking within early-age concrete due to thermal, drying and creep behavior. *Cement and concrete research*, *32*(7), 1053-1059.

[20] ACI Committee. (2007). ACI 207.2 R-07-Report on thermal and volume change effects on cracking of mass concrete. *American Concrete Institute, Farmington Hills*.

[21] NEVILLE, A. M. (2002). Properties of concrete.

[22] BENTZ, D. P. (2009). Early-age cracking review: mechanisms, material properties, and mitigation strategies. *Current Understanding of the Parameters that Influence Hydraulic and Leaching Properties and Uncertainty Analysis of Cementitious Barriers*, *901945*.

[23] WHITING, D. (1992). A Guide to Evaluating Thermal Effects in Concrete Pavements.

[24] NEVILLE, A. M. (2002). Properties of concrete.

[25] SCHINDLER, A. K., & FOLLIARD, K. J. (2003, August). Influence of supplementary cementing materials on the heat of hydration of concrete. In *Advances in cement and concrete IX conference, copper mountain conference resort in Colorado*.

[26] KLEMCZAK, B., & KNOPPIK-WRÓBEL, A. (2011). Early age thermal and shrinkage cracks in concrete structures–description of the problem. Architecture-Civil Engineering-Environment, 4(2), 35-48.

[27] FORTH, J. P., MARTIN, A., & ANCHOR, R. D. (2014). Design of liquid retaining concrete structures. Whittles Publishing.

[28] GILBERT, R. I. (2017). Cracking caused by early-age deformation of concrete–prediction and control. Procedia Engineering, 172, 13-22.

[29] ANCHOR RD. Design of liquid retaining concrete structures. (No Title). 1992 Jul.

[30] ACI Committee. (2007). ACI 207.2 R-07-Report on thermal and volume change effects on cracking of mass concrete. American Concrete Institute, Farmington Hills.

[31] BS 8007 :Design of concrete structures for retaining aqueous liquid, British Standards Institution. London, 1987.

[32] BS EN 1992-1: Eurocode 2: Design of concrete structures – Part 1: General requirements, British Standards Institution, London, 2004.

[33] ASTM C496. Standard Test Method for Splitting Tensile Strength of Cylindrical Concrete Specimens: ASTM International,2004.

[34] ASTM C39M-15a. Standard Test Method for Compressive Strength of Cylindrical Concrete Specimens.

[35] ASTM C78 / C78M-16. (2016). Standard Test Method for Flexural Strength of Concrete (Using Simple Beam with Third-Point Loading), ASTM International, West Conshohocken.

[36] BS EN 12390. (2000). Testing hardened concrete, method of determination of compressive strength of concrete cubes.

[37] European Committee for Standardization., & British Standards Institution 197-1. Cement. Part 1, Composition, specifications and conformity criteria for common cements. 2012.

[38] Iraqi Specification IQS No. 45. Aggregate from Natural Sources for Concrete and Construction. Central Agency for Standardization and Quality Control, Baghdad; 1984.

[39] ABDULMAJED, D. A. A., DAUD, S. A., & ALRSHOUDI, F. (2024). NUMERICAL VALIDATION OF LONG-TERM BEHAVIOUR OF REINFORCED RECYCLED AGGREGATE CONCRETE BEAM.

[40] TAHER, M. J., AL-ATTAR, T. S., & AL-ADILI, A. S. (2024). Compatibility and Mechanical Performance of High-Strength Self-Compacting Concrete Produced with Recycled Glass Powder. Civil and Environmental Engineering, 20(2), 1107-1119.

[41] AL-MASRAF, H. M., AL-ATTAR, T. S., & FREYYAH, Q. J. (2024). Fracture Behavior of Engineered Cementitious Composites Concrete Under Center Point Bending Load. Civil and Environmental Engineering, 20(2), 1002-1023.